

## SURFACE ENERGY OF SOLIDS: SELECTION OF EFFECTIVE SUBSTRATES FOR BIOADHESION IN AQUEOUS MEDIA

Katarzyna Boniewicz-Szmyt<sup>1\*</sup>, Stanisław J. Pogorzelski<sup>2</sup>

<sup>1</sup> Gdynia Maritime University, Morska 81-87, 81-225 Gdynia, Poland, Faculty of Marine Engineering, Department of Physics, ORCID 0000-0003-1693-6623, e-mail: k.boniewicz@wm.umg.edu.pl

<sup>2</sup> University of Gdańsk, Wita Stwosza 57, 80-308 Gdańsk, Poland, Faculty of Mathematics, Physics and Informatics, Institute of Experimental Physics, ORCID 0000-0001-5618-7941

\* Corresponding author

**Abstract:** Surface wettability of model solids of different hydrophobicity (from hydrophilic to hydrophobic) in contact with an aqueous medium was determined by measuring the dynamic contact angles (CA) using common techniques: sessile drop, inclined plate and captive bubble. The surface wettability energetics parameters: contact angle hysteresis (CAH), 2D adhesive layer pressure, surface free energy (SFE) and work values of cohesion, adhesion and spreading were determined using the formalism proposed by Chibowski [2003]. CA values depended on the technique used and experimental conditions (flow numbers, spatial heterogeneity and roughness of the sample). The most effective substrates for testing bioadhesion on solids submerged in aqueous media were hydrophilic surfaces (SFE ~ 40–58 mJ m<sup>-2</sup>; CAH ~ 16–20 mN m<sup>-1</sup>).

**Keywords:** wettability process energetics, surface adsorption, contact angle hysteresis, bioadhesion, surface energy.

### 1. INTRODUCTION

Wettability of solids and the related surface free energy (SFE) in contact with different liquids are highly relevant to such industrial processes as flotation, catalysis, or physicochemistry of coatings. There is a number of algorithms for determining SFE and its components using CA measurements [Żenkiewicz 2007], which lead to results dependent on the type of solid and properties of the test liquid used, experimental conditions, as well as the measurement technique type (sessile drop, inclined plate or captive bubble). Most solid surface energy theories are based on Young's equation and introduce an equilibrium contact angle  $\Theta_{eq}$ , with an exception being the contact angle hysteresis (CAH)-based formalism created by Chibowski [2003]. It introduces the dynamic contact angles  $\Theta_A$  and  $\Theta_R$ , and liquid surface tension  $\gamma_{LV}$  as input data for determining the wettability energy parameters.

In previous studies, a measurement system for *in situ* measurements of wetting properties of solids permanently submerged in water, which utilised the captive bubble method and proved optimal for studying bioadhesion under marine conditions [Pogorzelski, Mazurek and Szczepańska 2013]. This enables measuring fully hydrated, heterogeneous coating layers (biolayers) of solid substrates placed in liquid media (not necessarily aqueous), without any acquisition process or chemical interference with the structure of the test substrate, and the entirety of the fully automated, computer-controlled system is subject to a patent application [Pogorzelski and Grzegorzczuk 2016]. The purpose of this study was: to analyse the wettability parameters determined using different methods based on solid/liquid contact angle (CA) measurements for modelled substrates of varied physicochemical properties, and to select substrates for effective biomatter accumulation on solids.

The collected data will enable developing a methodology for assessing the properties of adhesive layers in materials engineering (hyrotechnical construction), shipbuilding (growths on submerged surfaces), and medicine (prosthetic materials – bacterial biolayers).

## 2. WETTABILITY OF SOLIDS – THEORETICAL BASICS

Wetting properties of surface-modified solids can be characterised in terms of a Young's static equilibrium contact angle, while changes in interaction energetics can be defined by determining free surface energy (using CA measurements), which plays a key role in describing physicochemical processes occurring at phase boundaries [Adamson and Gast 1997]. Wettability measurements are the most commonly used technique of surface examination, simple and sensitive, with an analysis depth of 0.5–1 nm [Strobel and Lyons 2011].

The static contact angle  $\Theta_{eq}$  is expressed by the free surface energies of three interphase surfaces, as shown in Figure 1, using the Young-Dupré equation [Lam et al. 2002]:

$$\gamma_{S/A} - \gamma_{W/S} = \gamma_{A/W} \cos\Theta_{eq}. \quad (1)$$

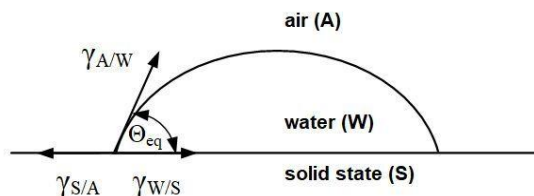


**Fig. 1.** Sessile drop at solid surface. Measurements of the equilibrium contact angle  $\Theta_{eq}$  from droplet contact line geometry and surface tension forces at three phase boundaries: air/water  $\gamma_{A/W}$ ; air/solid  $\gamma_{S/A}$ ; water/solid  $\gamma_{W/S}$

In practice, there are two dynamic contact angles measured at the same surface and for the same coating liquid, which depend on the movement of the liquid/solid contact line, as shown in Figure 2.

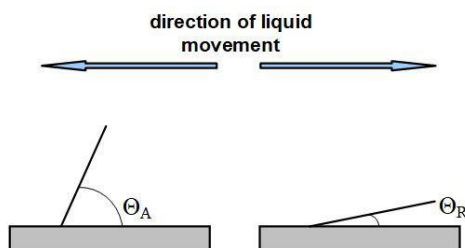


**Fig. 2.** Advancing  $\theta_A$  and receding  $\theta_R$  dynamic contact angles in the movement of liquid contact line along the solid surface

The difference between the advancing  $\Theta_A$  and receding angle  $\Theta_R$  is defined as the wetting angle hysteresis [Chibowski 2007]:

$$CAH = \Theta_A - \Theta_R. \quad (2)$$

Erbil et al. [1999] noted five causes for the occurrence of CAH: surface roughness, microscopic chemical heterogeneity, measurement droplet (or bubble) size, molecular reorientation at the surface, and liquid penetration into the solid surface.

On chemical heterogeneous surfaces,  $\Theta_A$  is a measure of wettability of the most hydrophobic component of the surface, while  $\Theta_R$  corresponds to the most hydrophilic component; the angles are related as follows:  $\Theta_A > \Theta_{eq} > \Theta_R$  [Adamson and Gast 1997]. It is often assumed that  $\Theta_{eq} = (\Theta_A + \Theta_R)/2$  is the mean value from both dynamic angles [Erbil 2006].

Young's equation is used for surfaces that are chemically homogeneous, smooth, flat, non-porous, non-absorbable, non-soluble, rigid, free of stresses, chemically non-reactive and remaining in a thermodynamic equilibrium with the surrounding environment [Tavana et al. 2004].

A number of formalisms have been developed for determining SFE and its components (responsible for individual interactions between liquid molecules and the surface) using CA measurements: Zisman method, equations of state, harmonic mean equations, geometric mean equations, and AB (acid-base) procedure (a review can be found in [Żenkiewicz 2007]). Most solid surface energy theories are based on Young's equation and introduce the equilibrium contact angle  $\Theta_{eq}$ .

An exception is the formalism developed by Chibowski [2003], where free surface energy  $\gamma_{SV}$  ( $= \gamma_{S/A}$  because gas media are not only air A, but also liquid

vapour V) and other parameters of surface wettability energetics: 2D surface pressure of the adhesive layer  $\Pi$ , adhesion work  $W_A$  and spreading work  $W_S$ , dispersion term  $\gamma_{SV}^d$  of total energy  $\gamma_{SV}$  are calculated from CAH using three measurable parameters: angles  $\Theta_A$  and  $\Theta_R$ , and surface tension of the test liquid  $\gamma_{LV}$ .

This model assumes that an additional factor causing CAH is a limited surface film left on the solid substrate as a result of adsorption or coating [Chibowski 2003]. A very good consistency has been achieved between surface energy values obtained using the CAH and AB methods for different surfaces [Radelczuk, Hołysz and Chibowski 2002].

The presence of the surface film leads to a change in free energy  $\gamma_{SV}$  of the solid, which is now  $\gamma_{SF}$ :

$$\gamma_{SF} = \gamma_{SV} + \Pi \quad (3)$$

$$\Pi = \gamma_{LV} (\cos \Theta_R - \cos \Theta_A), \quad (4)$$

where:  $\Pi$  is 2D surface pressure of the adsorbed film.

For Langmuir single-layer physical adsorption, Gibbs excess  $\Gamma$  (= number of moles of adsorbed substance per unit of area) equals  $\Gamma = \Pi/RT$ , where:  $R$  – gas constant and  $T$  – temperature [K]; Adamson and Gast [1997].

Total surface free energy  $\gamma_{SV}$  is defined by the following equation [Chibowski 2003]:

$$\gamma_{SV} = \Pi(1 + \cos \Theta_A)^2 / [(1 + \cos \Theta_R)^2 - (1 + \cos \Theta_A)^2]. \quad (5)$$

Work  $W_S$  of spreading a liquid on a solid is a thermodynamic quantity that defines a relation between wettability and mechanical force of adhesion, and is expressed by adhesion work  $W_A$  and cohesion work  $W_C$  [De Gennes 1985]:

$$W_S = W_A - W_C, \quad (6)$$

where:  $W_A = \gamma_{LV} (1 + \cos \Theta_A)$  and  $W_C = 2\gamma_{LV}$  [Adamson and Gast 1997]. (7)

Furthermore,  $W_S$  enables comparing liquid/solid adhesion forces for different liquids [Rodrigues-Valverde et al. 2002].

If no hysteresis ( $CAH=0$  and  $\Theta_{eq} = \Theta_A$ ) occurs in a liquid droplet/solid system, surface free energy is equal to half adhesion work  $W_A$ :

$$\gamma_{SV} = \frac{1}{2} \gamma_{LV} (1 + \cos \Theta_A) = \frac{W_A}{2}. \quad (8)$$

The dispersive interaction component  $\gamma_{SV}^d$  in total energy  $\gamma_{SV}$  results from the following relation [Chibowski 2003]:

$$\gamma_{SV}^d = \gamma_{LV} (1 + \cos\Theta_A)^2 / 4. \quad (9)$$

According to Van Oss [1997], in biological systems, hydrophobic London dispersion interactions are usually the strongest among all long-range, non-specific interactions, which are defined as attraction between non-polar or weakly polar molecules, particles or cells immersed in the aqueous phase.

Surface energy is represented as a sum of the dispersive and polar components, for surface interactions [Erbil 2006]:

$$\gamma_{SV} = \gamma_{SV}^d + \gamma_{SV}^p. \quad (10)$$

The proportion:

$$\frac{\gamma_{SV}^p}{\gamma_{SV}} = \left( \frac{\gamma_{SV} - \gamma_{SV}^d}{\gamma_{SV}} \right) 100 \text{ [in \%]} \quad (11)$$

is a polarity index of a solid in contact with the test liquid.

## 2.1. Optimum conditions for contact angle measurements

The classic hydrodynamic model of liquid movement on the surface of a solid, and of the interphase surface shape, indicates the conditions relevant to kinematic parameters, which enable achieving repeatable CA [Rame and Garoff 1996].

When considering a small liquid droplet of viscosity  $\mu$ , wetting a surface, we assume that its radius is smaller than the capillary length  $L_c$ :

$$L_c = \sqrt{\frac{\gamma}{\rho g}}, \quad (12)$$

where:  $\gamma$ ,  $\rho$  mean liquid surface tension and liquid density, respectively, while  $g$  is gravitational acceleration. For water,  $L_c \sim 2.7$  mm at  $T = 20$  °C.

The shape of a sessile drop can be approximated as a spherical cap, which corresponds to a thermodynamic equilibrium at a liquid/vapour interphase surface when the ratio of viscosity forces to capillary forces, given by capillary number  $Ca$ , is very low ( $10^{-3} \sim 10^{-5}$ ):

$$Ca \equiv \frac{u\mu}{\gamma}, \quad (13)$$

where:  $u$  is the specific rate of movement of the liquid-solid contact line front,  $\mu$  is liquid viscosity [Schaffer and Wong 2000].

In particular, dynamic contact angle  $\Theta_d$  depends on  $Ca$  in a manner shown by the following empirical relation [Bracke, De Voeght and Joos 1989]:

$$\cos\Theta_d = \cos\Theta_{eq} - 2(1 + \cos\Theta_{eq})Ca^{1/2}. \quad (14)$$

The liquid-solid contact line is well represented when: surface tension forces dominate over viscosity forces ( $Ca \ll 1$ ) and the force of gravity ( $Bd \ll 1$ ), where Bond number  $Bd$  is defined by the following relation:

$$Bd \equiv \frac{\rho g D^2}{\gamma}, \quad (15)$$

where:  $D$  is a characteristic length in the system (e.g. contact line length, droplet radius).

Weber number  $= \rho u^2 D / \gamma$  defines the ratio of inertia forces to capillary forces and should be  $\ll 1$ .

Fine surface irregularities  $< 0.5 \mu\text{m}$  have no significant impact on the  $CA$  values measured and calculated surface energy values [Qurynen and Bollen 1995].

## 2.2. Dynamic contact angle measurement methods

### 2.2.1. Expanding drop method

This method involves increasing and decreasing the volume of a droplet deposited on the surface of a solid (Fig. 3). During the first stage of the measurement the droplet front covers the test surface ( $\Theta_A$  is determined), then recedes, uncovering the surface covered previously ( $\Theta_R$  is determined).

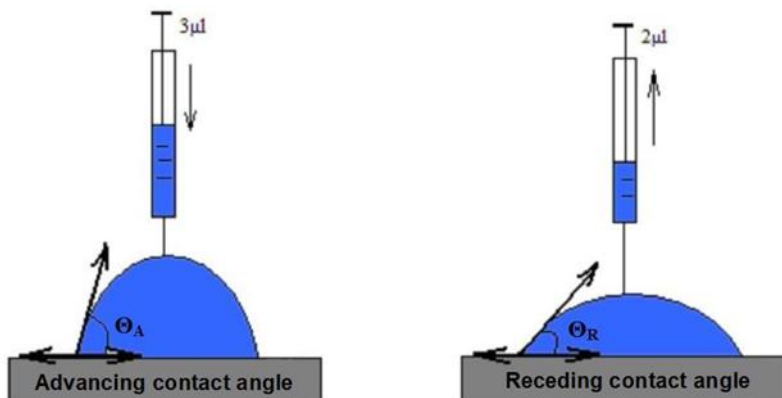


**Fig. 3.** Measuring the advancing and receding contact angle using the dynamic expanding drop method

### 2.2.2. Inclined plate method

CAH can be determined based on the shape of a droplet deposited on a flat solid surface with a varying angle of inclination relative to the horizontal plane [Lam et al. 2002]. By changing the inclination angle  $\Psi$  of the test material plate, angles  $\theta_A$  and  $\theta_R$  are read at the moment droplet movement begins (Fig. 4). The inclined plate method generates essentially identical  $\gamma_{SV}$  as the expanding drop method for model solids [Chibowski and Terpiłowski 2008].

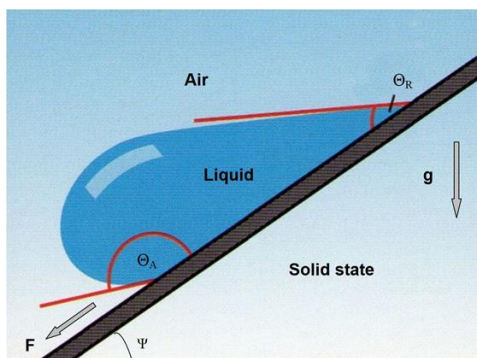


**Fig. 4.** Inclined plate method for  $CAH = \theta_A - \theta_R$  determination;  $\Psi$  – the critical angle of plate inclination at which the drop movement starts

### 2.2.3. Captive bubble method

A method for determining critical contact angles that utilises a deformation of an air bubble, which is formed at the tip of a dosing pipette and is in contact with a test surface immersed in water (Fig. 5).

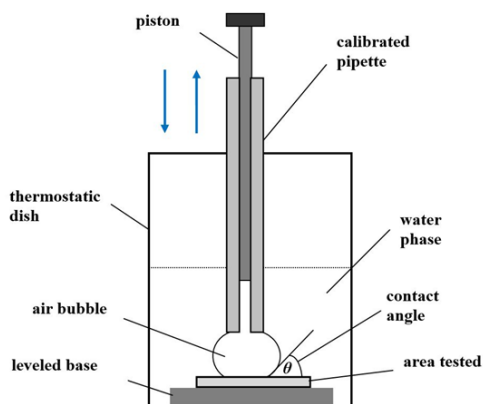


**Fig. 5.** Diagram of an experimental set-up for dynamic contact angle determination using the captive bubble method (modified after [Zhou et al. 1998])

This is the most common technique for studying wettability of immersed, biologically colonised solids [Pogorzelski, Mazurek and Szczepańska 2013], where hydrated, porous and heterogeneous structures enable the application of the sessile drop method. This method enables studying deposits *in situ*, providing repeatable CA values [Zhou et al. 1998]. The methodology has been successfully used to: determine changes in mineral wettability caused by adsorption of natural surfactants from seawater [Mazurek, Pogorzelski and Boniewicz-Szmyt 2009], control the effectiveness of liquids used for cleaning of dental prostheses [Pogorzelski et al. 2012], microorganisms bioadhesion to immersed artificial substrates [Pogorzelski, Mazurek and Szczepańska 2013], and monitor the surface erosion of needles, caused by atmospheric pollution [Pogorzelski, Rochowski and Szurkowski 2014].

### 3. STUDY METHODOLOGY

#### 3.1. Test material

To characterise the surface wettability parameters of model artificial and natural substrates in terms of their ability to accumulate biofilms, CA measurements were performed on a broad group of solids: polymers, metals, rubber, glass, composite and gel materials, all with different hydrophobicity properties in contact with distilled water obtained from a deionisation apparatus (Millipore, conductivity =  $0.05 \mu\text{S cm}^{-1}$ ) with pH  $5.8 \pm 0.1$  and surface tension  $\gamma_{LV} = 71.1 \pm 0.2 \text{ mN m}^{-1}$  at room temperature  $T = 22 \text{ }^\circ\text{C}$ .

#### 3.2. CA measurement methods

Diagrams of the measurement systems used to determine the solid/liquid dynamic contact angles, including details on the measurement procedure for the three techniques applied are presented in Section 3 in the paper [Mazurek, Pogorzelski and Boniewicz-Szmyt 2009]. Depending on the variant of the method used, a plate with a liquid droplet (sessile drop method), a plate with a droplet on an adjustable tilt base (inclined plate method), or a cuvette with a calibration pipette (captive bubble method) is placed in the image registration path between the illuminator (a wide beam of scattered light) and the camera.

Figure 6 shows a prototype measurement system developed for field measurements, based on the latter CA measurement method, while the conditions of the experiment and the measurement track elements used are discussed in detail in [Pogorzelski, Mazurek and Szczepańska 2013]. A cuboid vessel with transparent walls (PMMA) is filled with water. Plates made of model materials (dimensions



77 x 26 x 1 mm, typical for glass microscope plates) were used as the artificial substrates. In the aqueous phase is placed an automatic calibration pipette (25  $\mu$ l without the dosing tip), at the end of which a bubble with a 3–6 mm diameter and constant volume is formed. The bubble is pressed against the sample surface, which enables determining the contact angle  $\Theta_R$ . Next, the stand's movement is reversed, and the bubble is pulled away from the test substrate, and the second angle  $\Theta_A$  is measured. The image is recorded with a microscope camera, saved on a computer and subsequently analysed with graphics software (ImageJ). CA is read multiple times (5–10) on both sides of the contact line, which eliminates the impact of sample inclination or deformation. The accuracy of an individual CA measurement is  $0.1^\circ$ , while result repeatability is at the order of  $0.4^\circ$ . The pipette-holding stand enables selecting the test surfaces in the x-y plane. A digital microscope camera with a periscope enables recording the image of the bubble in contact with the test surface and does not require a measurement vessel, but only a firm mounting to the ground at the measurement site. Samples with adhesive layers (microorganism films) are mounted to the base that combines the periscope and camera stand into a whole.



**Fig. 6.** Experimental set-up for dynamic contact angle determination on submerged solid surfaces designed for field work

Automated CA measurements are enabled with a modified computer-controlled version of the device, which is subject to a patent submission [Pogorzelski and Grzegorzczuk 2016].

## 4. RESULTS AND DISCUSSION

### 4.1. Surface wettability parameters

Example recordings of the shape of interphase surfaces and the method of determining dynamic CA values using the inclined plate and captive bubble methods are shown in Figures 7a and 7b, respectively, for the same material (poly(methyl methacrylate), PMMA).

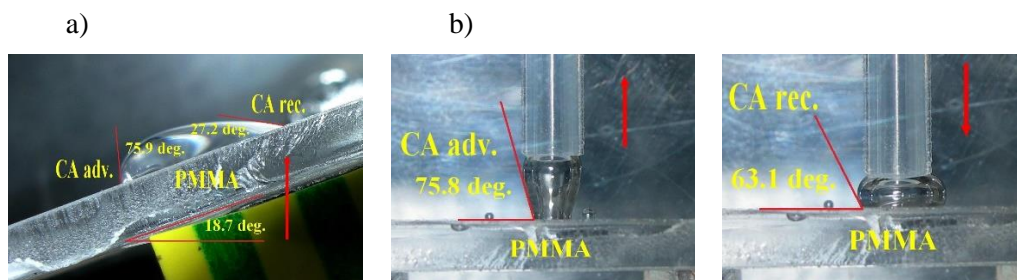


**Fig. 7.** Example images of interphase surface shapes as a basis for dynamic CA determination with the inclined plate a) and captive bubble b) methods, for PMMA substrates

Table 1 summarises the surface wettability parameters of model solids.  $\theta_A$  values measured using the inclined plate method are higher by several degrees, while  $\theta_R$  lower by several degrees from those obtained using the captive bubble and sessile drop methods; similar results were found in earlier studies [Rymuszka, Terpiłowski and Hołysz 2013]. A similar divergence was found for mineral surfaces in contact with seawater from natural bodies of water [Mazurek, Pogorzelski and Boniewicz-Szmyt 2009]. This leads to overestimated CAH values and higher  $\Pi$ ,  $\gamma_{SV}$ ,  $W_S$ ,  $W_A$  than in the bubble method. The difference diminishes to a few percent for hydrophobic materials (wax, polymers, gel materials). In methods based on sessile drop geometry, the basic condition of thermodynamic equilibrium at the surface between the liquid and the gaseous phase (or specifically the liquid's vapour) is not met. The volume of gas trapped in the bubble, surrounded by the aqueous phase, enables achieving the state of saturated vapour and obtaining reliable CA values only in the captive bubble method. Interim processes occurring at the surface during the measurement (e.g. swelling for gel samples, item 12 in Table 1 can lead to materially inconsistent values of parameters that depend on the

CA measurement method used. Hydrophobic surfaces are characterised by low  $\gamma_{SV}$  and CAH, and high  $\theta_A$  and  $\theta_R$ , with a contribution of the dispersion component  $\gamma_{SV}^d/\gamma_{SV}$  at the order of 0.68 to 0.76. Hydrophilic substrates (glass, metals) possess higher  $\gamma_{SV}$  (within the 40–58  $\text{mJ m}^{-2}$  range), while exhibiting lower CA and  $\gamma_{SV}^d/\gamma_{SV}$ . Surface energy  $\gamma_{SV}$  can be calculated, assuming no CA hysteresis, from equation (8), assuming  $\Theta_{eq} = 31.80^\circ$  for glass, which leads to the value of 67.79  $\text{mJ m}^{-2}$ . It is much higher than that obtained from dynamic CA measurements ( $\gamma_{SV} = 54.49 \text{ mJ m}^{-2}$ ), which is consistent with literature data for glass surfaces [Jańczuk, Wójcik and Zdziennicka 1999]. Introduction of additives to the base material, in the form of dyes (compare 2–4 in Table 1 for PVC film) leads to significant changes of wettability parameters (as much as 14% for  $\gamma_{SV}$ ). Even the form and manner of surface preparation (rolling, stretching) have a substantial impact on wettability parameters, which is demonstrated when data for the same material (Al) are compared in the case of its foil or a rolled layer (compare 6 and 11 in Table 1).

**Table 1.** Wettability parameters of solids in contact with distilled water ( $\gamma_{LV} = 71.1 \text{ mN m}^{-1}$ ;  $T = 22 \text{ }^\circ\text{C}$ ); CA determination methods: S – sessile drop (horizontal surface – static CA measurement), N – inclined plate, P – captive bubble

No.	Solid	$\Theta_A$	$\Theta_R$	CAH	$\Pi$	$\gamma_{SV}$	$W_A$	$W_S$	$\Theta_{eq}$	$\gamma_{SV}^d$	Method
		[°]	[°]	[°]	[ $\text{mN m}^{-1}$ ]	[ $\text{mJ m}^{-2}$ ]	[ $\text{mJ m}^{-2}$ ]	[ $\text{mJ m}^{-2}$ ]	[°]	[ $\text{mJ m}^{-2}$ ]	
1	Clean glass	-	-	0	0	67.7	135.5	-11.0	31.8	-	S
	Clean glass	50.1	11.5	38.6	24.8	54.4	120.2	-26.3	31.8	49.3	P
2	Red PVC film	79.2	30.2	49.5	48.2	32.8	84.4	-57.8	54.7	25.0	N
		88.5	69.8	18.6	22.7	31.5	73.0	-69.2	79.1	18.7	P
3	Brown PVC film	77.8	27.1	50.7	48.3	33.6	86.1	-56.1	52.5	26.0	N
		77.3	55.9	21.4	24.3	38.0	86.7	-55.5	66.6	26.4	P
4	Orange PVC film	86.4	30.1	56.3	57.1	27.4	75.5	-66.7	58.2	20.0	N
		91.4	65.6	25.8	31.1	28.2	69.3	-72.9	78.5	16.8	P
5	Gum	88.0	22.8	65.2	63.2	25.6	73.5	-68.7	55.4	18.9	N
		75.0	47.5	27.5	29.6	38.3	89.5	-52.7	61.2	28.1	P
6	AL foil	83.5	30.7	58.8	53.1	29.6	79.1	-63.1	57.1	21.9	N
		92.6	82.4	10.1	12.6	31.0	67.8	-74.4	87.5	16.1	P
7	Galvanized steel	75.2	25.0	50.2	46.3	35.4	89.2	-53.0	50.1	27.9	N
		80.7	52.8	27.8	31.5	34.6	82.5	-59.7	66.7	23.9	P
8	Paraffin wax	100.3	70.8	29.5	36.1	22.2	58.3	-83.9	85.5	11.9	N
		101.5	91.2	10.3	12.8	25.5	56.8	-85.4	96.4	11.3	P
9	Teflon PTFE	105.1	58.4	46.7	55.8	17.1	52.5	-89.7	97.1	9.6	N
		106.7	79.2	27.5	33.8	18.9	50.6	-91.6	93.0	9.0	P
10	Plexi PMMA	86.1	27.5	58.5	58.2	27.4	75.9	-66.3	77.2	20.2	N
		85.0	67.4	17.6	21.2	33.9	77.2	-65.0	76.2	20.9	P
11	AL plate	74.1	17.2	56.8	48.4	35.7	90.6	-51.6	64.9	28.8	N
		81.8	68.9	16.9	20.4	33.6	76.2	-66.0	75.4	23.1	P
12	Gel surface	98.3	31.7	66.6	70.8	19.1	60.7	-81.5	70.9	12.9	N
		82.7	77.9	4.7	5.8	38.6	80.1	-62.1	76.8	22.5	P

In the model study discussed, distilled water was used, while seawater from natural water bodies in addition to a mixture of electrolyte contains natural surface active substances (surfactants). The latter, by being adsorbed on the interphase liquid droplet placed on the solid surface, form a hydrophobic barrier [Afsar-Siddiqui, Luckham and Matar 2003], which leads to CA values being 5–15° higher

for seawater as compared to distilled water [Mazurek, Pogorzelski and Boniewicz-Szmyt 2009]. The surface charge, formed due to the presence of electrolytes, is mainly a function of pH. Karaguzel et al. [2005] demonstrated that a NaCl addition ( $\ll 1 \text{ mol dm}^{-3}$ ) leads to a change in CA by less than  $3\text{--}4^\circ$ . It should be noted that Baltic water salinity is much lower ( $5\text{--}7 \text{ PSU}$ ) than that of standard artificial seawater ( $\sim 35 \text{ PSU}$ ), thus the electrolyte effect may not have a substantial impact on the measured CA values.

## 4.2. Wettability and adhesion properties

The impact of surface energy on bioadhesion has been studied using various materials, from urethanes and epoxides (with high  $\gamma_{SV}$ ) to silicones and hydrogen halides (with low  $\gamma_{SV}$ ; [Finlay et al. 2002]). Generally, hydrophobic surfaces exhibit a tendency to adsorb proteins and polymer materials from aqueous media, while hydrophilic ones more effectively gather polar and charged materials. Baier [1980] demonstrated a connection between bioadhesion and surface energy of the substrate. He found the existence of a window in surface energy (between  $20\text{--}30 \text{ mJ m}^{-2}$ ), where adhesion reaches a minimum. Substrates having a  $\gamma_{SV}$  below 20 and above  $30 \text{ mJ m}^{-2}$  display a substantial accumulation of biomass, with a maximum for surfaces with energies of approximately  $60 \text{ mJ m}^{-2}$  [Baier 2006]. Table 1 indicates that polymers, wax layers, rubber and gel materials, as hydrophobic bodies of low  $\gamma_{SV}$  and high CA values, do not constitute effective deposition substrates for biofilms, but may find use as coatings preventing the overgrowth of submerged surfaces with microorganism colonies, e.g. in hydrotechnical structures or shipbuilding. The test hydrophilic substrates (glass, metals, wood), possessing higher  $\gamma_{SV}$  (within the  $40\text{--}58 \text{ mJ m}^{-2}$  range) and lower CA and  $\gamma_{SV}^d/\gamma_{SV}$ , exhibit a high capacity for bioaccumulation. In addition to SFE, other factors as well [Batlin et al. 2003], such as surface charge, scale of surface irregularity, temperature, shearing stress of liquid flow, and the presence of surfactants, can substantially affect bioadhesion effectiveness [Zhao et al. 2005; Thomas and Muirhead 2009]. There are few studies of the effect of substrate colour on microorganism adhesion ability [Robson et al. 2009]. For polymer substrates with  $\gamma_{SV}$  within the range  $18\text{--}40 \text{ mJ m}^{-2}$ , it was found [Lakshmi et al. 2012], that biomatter accumulation is positively correlated with  $\gamma_{SV}$  ( $R = 0.66$ ). Schmidt et al. [2004] confirmed that biofilm adhesion ability is not exclusively correlated with SFE, but rather with CAH. Coating layers that are the most weakly bound to the substrate are characterised by the lowest CAH values, and CAH increase is coupled with an increase in liquid/solid adhesion force. Surface bioadhesion leads to a hydrophobisation of the surface ( $\theta_{eq}\uparrow$ ,  $\theta_A\uparrow$ ,  $\theta_R\uparrow$ ,  $CAH\downarrow$ ,  $\gamma_{SV}\downarrow$ ,  $W_A\downarrow$ , while  $W_S$  is more negative, and  $\gamma_{SV}^d/\gamma_{SV}\downarrow$ ).

The variation in the wettability of the studied substrates becomes more clearly visible if CAH is shown as a function of  $W_S$  [Pogorzelski, Rochowski and

Szurkowski 2014]. CAH depends on the physical properties of the solid/liquid contact surface (spatial irregularity and heterogeneity), while  $W_S$  on the chemical nature of the liquid ( $\gamma_{LV}$ ) and solid ( $\gamma_{SV}$ ) materials in contact with each other. Having similar CAH, metals are more hydrophilic than polymers (less negative  $W_S$ ). On the other hand, natural substrates with similar  $W_S$  as metals, have CAH 2–3 times lower than metals [Mazurek, Pogorzelski and Boniewicz-Szmyt 2009; Pogorzelski, Mazurek and Szczepańska 2013].

## 5. CONCLUSIONS

Systematic differences in the values of wettability parameters of model solids obtained from the Chibowski formalism [2003] using three techniques of dynamic contact angle measurement.  $\theta_A$  values measured using the inclined plate method are higher by several degrees, while  $\theta_R$  lower by several degrees from those obtained using the captive bubble and sessile drop methods; which leads to an overestimation of the other wetting energetics parameters: CAH, elevated  $\Pi$ ,  $\gamma_{SV}$ ,  $W_S$ ,  $W_A$ . The differences result from different thermodynamic conditions of the wetting process.

The measurement set-up for determining dynamic CA values, based on captive bubble geometry, provided reliable results in *in situ* tests of hydrated, heterogeneous surfaces permanently immersed in liquids, without interference in the structure of the surface layer or a need to use a number of test liquids.

The surface parameters that proved decisive for the intensity of bioadhesion to solid beds immersed in water were SFE and CAH. The highest bioaccumulation of hydrophilic material is exhibited by substrates with SFE  $\sim 40$ – $58 \text{ mJ m}^{-2}$  and CAH  $\sim 16$ – $20 \text{ mN m}^{-1}$ .

An automated version of the measurement system and the results presented herein find broad use in testing the adhesive properties of substrates important to industry (anti-corrosive coatings, paint coatings), shipbuilding (systems preventing submerged surface overgrowth), hydrotechnical construction, medicine (prosthetic materials resistant to bacterial colonisation), etc.

## REFERENCES

- Adamson, A.W., Gast, A.P., 1997, *Physical Chemistry of Surfaces*, 6th edition, Wiley and Sons, New York, USA.
- Afsar-Siddiqui, A.B., Luckham, P.F., Matar, O.K., 2003, *The Spreading of Surfactant Solutions on thin Liquid Films*, Adv. Colloid Interf., vol. 106, pp. 183–236.

- Baier, R.E., 1980, *Adsorption of Microorganisms to Surface*, Wiley-Interscience Publishers, New York, USA, pp. 59–104.
- Baier, R.E., 2006, *Surface Behaviour of Biomaterials: The Theta Surface for Biocompatibility*, J. Mater. Sci.: Mater. Med., vol. 17, pp. 1057–1062.
- Batlin, T.J., Kaplan, L.A., Newbold, J.D., Cheng, X., Hansen, C., 2003, *Effects of Current Velocity on the Nascent Architecture of Stream Microbial Biofilms*, Applied and Environmental Microbiology, vol. 69, pp. 5443–5452.
- Bormashenko, E., Bormashenko, Y., Whyman, G., Pogreb, R., Musin, A., Jager, R., Barkay, Z., 2008, *Contact Angle Hysteresis on Polymer Substrates Established with Various Experimental Techniques, its Interpretation, and Quantitative Characterization*, Langmuir, vol. 24, pp. 4020–4025.
- Bracke, M., De Voeght, F., Joos, P., 1989, *The Kinetics of Wetting: the Dynamic Contact Angle*, Progress in Colloid & Polymer Science, vol. 79, pp. 142–149.
- Chibowski, E., 2003, *Surface Free Energy of a Solid from Contact Angle Hysteresis*, Adv. Colloid Interf. Sci., vol. 103, pp. 149–172.
- Chibowski, E., 2007, *On Some Relations Between Advancing, Receding and Young's Contact Angles*, Adv. Colloid Interf. Sci., vol. 133, pp. 51–59.
- Chibowski, E., Terpiłowski, K., 2008, *Surface Free Energy of Sulfur – Revisited I. Yellow and Orange Samples Solidified Against Glass Surface*, J. Colloid. Interface Sci., vol. 319, pp. 505–513.
- De Gennes, P.G., 1985, *Wetting: Statics and Dynamics*, Review of Modern Phys., vol. 57, pp. 827–834.
- Drelich, J., Miller, J.D., Good, R.J., 1996, *The Effect of Drop (Bubble) on Advancing and Receding Contact Angles for Heterogenous and Rough Solid Surfaces as Observed with Sessile-drop and Captive-bubble Techniques*, Journal of Colloid and Interface Science, vol. 179, pp. 37–50.
- Erbil, H.Y., 2006, *Surface Chemistry of Solid and Liquid Interfaces*, Blackwell Publ. Ltd., Hong Kong.
- Erbil, H.Y., Mc Hale, G., Rowan, S.M., Newton, M.I., 1999, *Determination of the Receding Contact Angle of Sessile Drops on Polymer Surfaces*, Langmuir, vol. 15, pp. 7378–7385.
- Finlay, J.A., Callow, M.E., Ista, L.K., Lopez, G.P., Callow, J.A., 2002, *The Influence of Surface Wettability on the Adhesion Strength of Settled spores of the Green Alga Enteromorpha and the Diatom Amphora*, Integr. Comp. Biol., vol. 42, pp. 1116–1122.
- Jańczuk, B., Wójcik, W., Zdziennicka, A., 1999, *Wettability and Surface Free Energy of Glass in the Presence of Cetyltrimethylammonium Bromide*, Materials Chemistry and Physics, vol. 58, pp. 166–171.
- Karaguzel, C., Can, M.F., Sonmez, E., Celik, M.S., 2005, *Effect of Electrolite on Surface Free Energy Components of Feldspar Minerals Using Thin-layer Wicking Method*, J. Colloid Interface Sci., vol. 285, pp. 192–200.
- Lakshmi, K., Muthukumar, T., Doble, M., Vedaprakash, L., Kruparathnam, D., Dineshram, R., Jayaraj, K., Venkatesan, R., 2012, *Influence of Surface Characteristics on Biofouling Formed on Polymers Exposed to Coastal Sea Waters of India*, Colloids and Surfaces B: Biointerfaces, vol. 91, pp. 205–211.
- Lam, C.N.C., Wu, R., Li, D., Hair, M.L., Neumann, A.W., 2002, *Study of the Advancing and Receding Contact Angles: Liquid Sorption as a Cause of Contact Angle Hysteresis*, Advances in Colloid and Interface Science, vol. 96, pp. 169–191.

- Mazurek, A., Pogorzelski, S.J., Boniewicz-Szmyt, K., 2009, *Adsorption of Natural Surfactants Present in Sea Waters at Surfaces of Minerals: Contact Angle Measurements*, *Oceanologia*, vol. 51, pp. 377–403.
- Pogorzelski, S.J., Berezowski, Z., Rochowski, P., Szurkowski, J., 2012, *A Novel Methodology Based on Contact Angle Hysteresis Approach for Surface Changes Monitoring in Model PMMA-Corega Tab System*, *Applied Surface Science*, vol. 258, pp. 3652–3658.
- Pogorzelski, S.J., Grzegorzczak, M., 2016, *Method and Automatic Device for Continuous Non-invasive Measurement of Surface Energy of Solids Permanently Immersed in Liquids*, Polish Government Patent Office, submission no. P.419913, University of Gdańsk, Gdańsk, Poland.
- Pogorzelski, S.J., Mazurek, A.Z., Szczepańska, A., 2013, *In-situ Surface Wettability Parameters of Submerged in Brackish Water Surfaces Derived from Captive Bubble Contact Angle Studies as Indicators of Surface Condition Level*, *Journal of Marine Systems*, vol. 119–120, pp. 50–60.
- Pogorzelski, S.J., Rochowski, P., Szurkowski, J., 2014, *Pinus sylvestris L. Needles Surface Wettability Parameters as Indicators of Atmospheric Environment Pollution Impacts: Novel Contact Angle Hysteresis Methodology*, *Applied Surface Science*, vol. 292, pp. 857–866.
- Radelczuk, H., Hołysz, L., Chibowski, E., 2002, *Comparison of the Lifshits – Van der Waals/Acid Base and Contact Angle Hysteresis Approaches to Determination of the Solid Surface Free Energy*, *Journal of Adhesion Science and Technology*, vol. 16, pp. 1547–1568.
- Rame, E., Garoff, S., 1996, *Microscopic and Macroscopic Dynamic Interface Shapes and the Interpretation of Dynamic Contact Angles*, *Journal of Colloid and Interface Science*, vol. 177, pp. 234–244.
- Robson, M.A., Williams, D., Wolff, K., Thomason, J.C., 2009, *The Effect of Surface Colour on the Adhesion Strength of *Elminus Modestus* Darwin on a Commercial Non-biocidal Antifouling Coating at Two Locations in the UK*, *Biofouling*, vol. 25, pp. 215–227.
- Rodrigues-Valverde, M.A., Cabrerizo-Vilches, M.A., Rosales-Lopez, P., Paez-Duneas, A., Hidalgo-Alvarez, R., 2002, *Contact Angle Measurements on Two (Wood and Stone) Non-ideal Surfaces*, *Colloids and Surfaces. A: Physicochem. Eng. Aspects*, vol. 206, pp. 485–495.
- Rymuszka, D., Terpiłowski, K., Hołysz, L., 2013, *Influence of Volume Drop on Surface Free Energy of Glass*, *Annales Univ. Mariae Curie-Skłodowska Lublin*, vol. LXVIII, Sec. AA, pp. 121–132.
- Schaffer, E., Wong, P., 2000, *Contact Line Dynamics Near the Pinning Threshold: A Capillary Rise and Fall Experiment*, *Physical Review E*, vol. 61, pp. 5257–5277.
- Schmidt, D.L., Brady, R.F., Lam, K., Schmidt, D.C., Chaudhury, M.K., 2004, *Contact Angle Hysteresis, Adhesion, and Marine Biofouling*, *Langmuir*, vol. 20, pp. 2830–2836.
- Strobel, M., Lyons, Ch.S., 2011, *An Essay on Contact Angle Measurements*, *Plasma Process. Polym.*, vol. 8, pp. 8–13.
- Qurynen, M., Bollen, C.M., 1995, *The Influence of Surface Roughness and Surface Free- Energy on Supra- and Subgingival Plaque Formation in Man*, *J. Clin. Periodontol.*, vol. 22, pp. 1–14.
- Tavana, H., Lam, C.N.C., Grundke, K., Friedel, P., Kwok, D.Y., Hair, M.L., 2004, *Contact Angle Measurements with Liquids Consisting of Bulky Molecules*, *J. Colloid Interf. Sci.*, vol. 279, pp. 493–502.
- Thomas, E., Muirhead, D., 2009, *Impact of Wastewater Fouling on Contact Angle*, *Biofouling*, vol. 25, pp. 445–454.
- Van Oss, C.J., 1997, *Hydrophobicity and Hydrophilicity of Biointerfaces*, *Current Opinion in Colloid and Interface Science*, vol. 2, pp. 503–512.
- Zhao, Q., Liu, Y., Wang, C., Wang, S., Muller-Steinhagen, H., 2005, *Effect of Surface Free Energy on the Adhesion of Biofouling and Crystalline Fouling*, *Chemical Engineering Science*, vol. 60, pp. 4858–4865.

- Zhou, Z.A., Hussein, H., Xu Z., Czarnecki, J., Masliyah, J.H., 1998, *Interaction of Ionic Species and Fine Solids with a Low Energy Hydrophobic Surface from Contact Angle Measurement*, J. Colloid Interface Sci., vol. 204, pp. 342–349.
- Żenkiewicz, M., 2007, *Methods for the Calculation of Surface Free Energy of Solids*, Journal of Achievements in Materials and Manufacturing, vol. 24, pp. 137–145.